Journal of the Korean Nuclear Society
Volume 23, Number 3, September 1991

Defect Model for the Oxygen Potential of Urania doped wit Gadolinia

Kwang Heon Park and Jang Wook Kim
Kyunghee University
(Received January 7, 1991)

가돌리니아 첨가 이산화우라늄의 점결함 모델에 의한 산소포텐샬 연구

박광헌 · 김장욱
경희대학교
(1991. 1. 7 접수)

Abstract

A defect model explaining the oxygen potential of Gadolinia doped urania based on the defect structure of pure urania has been developed. Gd-dopants are assumed to stay in the cation sites pushing away nearby oxygen interstitials reducing the number of interstitial sites. Gd-dopants also form dopant-vacancy clusters in the abundance of oxygen vacancies. This model explains the discontinuous change of the oxygen potential at O/M= as well as the increase of the potential with the dopant concentration.

요 약

가돌리니아 첨가 우라니아에 대한 점결함 모델이 순수 우라니아의 점결함구조를 바탕으로 하여 개발되었다. Gd 도펀트는 금속이온자리에 −1의 유효전하를 지니고, 주위의 산소침입형을 밀어내어 산소침입형의 자리를 감소시킨다. 산소 공공 농도가 증가하면 Gd 도펀트는 산소공공과 집합체를 형성하게 된다. 이 점결함 모델은 Gd 도펀트의 양의 증가에 따른 산소포텐샬의 증가와 산소 대 금속비율이 2일때 급속한 산소포텐샬 변화를 설명하여, 현존하는 실험값과 좋은 일치를 보였다.

I. Introduction

Thermochemistry of uranium oxide containing rare-earth cations is important in nuclear oxide fuel technology. Many fission products are the lanthanindes in the UO_2 fuel, and Gd-doped urania(GDU) is used as a fuel for a burnable-neutron-poison in a nuclear reactor[1].

While its many engineering characteristics are relatively well known [2,3], the elementary knowledge of GDU, especially defect structures and explanations for the oxygen potential, has not yet come. Oxygen potential, a kind of the chemical potential of oxygen in oxides, is an important parameter in characterizing the fuel performance during operation, and in controlling the stoichiometry of urania during sintering of fuel pellets. Oxygen potential is also an indirect indicator in finding the defect structure of the oxide[4].

Several simple defect models were tried for the mixed oxide such as (Pu, U)O_2 [5,6]. Assuming that Pu exists as Pu–anion vacancy clusters, a simple expression for the oxygen potential was successfully obtained[6]. Nowadays, more complex analyses (statistically oriented) are available [7,8] ; but, they are so far successful only for (Pu,U)O_2.

One of difficulties of applying the defect model to the doped urania was unavailability of a correct set of the basic defect (including clusters) equilibrium interrelations in both hypo– and hyper-stoichiometric pure urania. Park and Olander developed a defect model of pure uranium dioxide incorporating defect clusters, and the oxygen potential from this defect model well represents the experimental behavior in the range of $UO_{2.1}$ and $UO_{1.9}$[9]

The oxygen potential of urania increases with the addition of gadolinia ; however, the abrupt change of the potential still occurs at the exact stoichiometry, i.e., O/M ratio=2. Hence, any model developed should explains these behaviors. Une and Oguma's model is successful only for the explanation of the former[10]. In this paper, the oxygen potential of GDU is explored from the defect model of pure urania developed by Park and Olander[9], assigning the appropriated extrinsic defects formed by dopants and the defects originally exist in pure urania.

Ⅱ. Review:Defect Structure of Pure Urania[9]

The point defects are assumed to interact with each other in an ideal manner. The concentrations of some defects may increase with non–stoichiometry, until the ideality no longer prevails. These point defects form short–range clusters. So, the difficulty of treating non–ideality can be cleared by the introduction of these defect clusters(e.g., Willis defect) as point defects.

Table 1 summarizes the defect types used in the analysis of pure urania. Kroeger and Vink's notation for the point defects are used.

Table 1. The Defects and Clusters Used in the Pure Urania Modal

Notation	Definition	Effectie Charge
O_i''	Oxygen Interstitial	−2
$V_o^{\cdot\cdot}$	Oxygen Vacancy	+2
U'	(Negative) Polaron	−1
$U^{\cdot}$	Hole	+1
$(2:2:2)'$	Willis Defect	−1
$(V:U:V)^{\cdot\cdot}$	Vacancy Dimer	+2

The effective charge is defined as the difference of the ionic state of the defect from that of the original atom on the site which is now occupied by the defect.

Table 2 shows the defect relatons in pure urania. The REDOX equilibria which relate the oxygen potential with the concentration of the oxygen interstitials or vacancies are given in eq.(1) and (2). The formation of a Willis cluster and a dimer are indicated in eq.(3) and (4), respectively. The Frenkel pair formation (eq.(6)) and the disproportionation of U (eq.(5)) are also given. The relations, obtained when the mass action law was applied to each reaction in Table 2, are shown in Table 3.

Table 2. The Defect Relations in Pure Urania.

$2\,U_u^x + 1/2\,O_2(g) = O_i'' + 2\,U^{\cdot}$	(1)
$2\,U_u^x + O_o^x = 1/2\,O_2(g) + V_o^{\cdot\cdot} + 2\,U'$	(2)
$2\,O_o^x + 2\,O_i'' + 3\,U^{\cdot} = (2:2:2)' + 3\,U_u^x$	(3)
$2\,V_o^{\cdot\cdot} + 2\,U' = (V:U:V)^{\cdot\cdot} + U_u^x$	(4)
$2\,U_u^x = U^{\cdot} + U'$	(5)
$O_o^x = O_i'' + V_o^{\cdot\cdot}$	(6)

The six equilibrium constants were determined from fitting to the experimental data of pure urania[9]. The enthalpy and the entropy changes of each reaction are in Table 4. The exact values of K_F were not determined due to the lack of ex-

Table 3. Defect Relations after Applying the Mass Action Law.

$$\frac{[O_i''][U^{\cdot}]^2}{[U_u^x](P_o)^{1/2}}=K_{OX} \quad (7)$$

$$\frac{(P_o)^{1/2}[V_o^{\cdot\cdot}][U']^2}{[U_u^x]^2[O_o^x]}=K_{RE} \quad (8)$$

$$\frac{[(2:2:2)'][U_u^x]^3}{[O_o^x]^2[O_i'']^2[U]^3}=K_C \quad (9)$$

$$\frac{[U_u^x][(V:U:V)^{\cdot\cdot}]}{[V_o]^2[U']^2}=K_{CV} \quad (10)$$

$$\frac{[U'][U^{\cdot}]}{[U_u^x]^2}=K_E \quad (11)$$

$$\frac{[O_i''][V_o^{\cdot\cdot}]}{[O_o^x]}=K_F \quad (12)$$

perimental data. A series of pairs of entropy and enthalpy ranging (-3cak/mol-K, 77kcal/mol) to (6cal/mol-K, 94kcal/mol) were obtained for K_F.

Table 4. The Equilibrium Constants of the Defect Relations

Equil. Constant	ΔS°(cal/mol-K)	ΔH°(kcal/mol)
K_C	52	26
K_{OX}	-44	-50
K_{RE}	29	199
K_{CV}	-10	-82

Ⅱ. Point Defect Structure in GDU

Since the oxygen potential increases with the Gd dopant concentration, the defect structure of GDU should be different from that of pure urania. However, the basic structure of the mixture still remains as a fluorite with the addition of small amount of gadolinia. Based on this fact, we assume that the elementary defects in pure urania also exist in doped urania, and the defect relations in Table 2 are also applicable to GDU.

Trivalent Gd exists in the oxide as an isolated defect on the cation sublattice(Gd_U), unless anion vacancies exist. Because of its negative effective charge(-1), this cation repels nearby negatively-charged oxygen interstitials(O_i''), eliminating a certain number of the sites for the anion interstitials.

In the pure urania study[9], the concentration of oxygen interstitials was defined with respect to the number of cation lattice sites. This is called the absolute defect concentration($[O_i'']$). In the fluorite structure, an oxygen interstitial stays in the empty center of the cube formed by eight anions. Hence, the number of the sites of oxygen interstitials in pure urania is 1, and the fraction of the interstitials occupying this site is the absolute concentration. When the trivalent cation blocks a certain number of neighboring interstitial sites from occupancy by oxygen interstitials, the number of lattice sites decreases, which appears in the mass action laws involving O_i'' as an increase in the concentration of this species for the same number per unit volume. The appropriate concentration for this purpose is the chemical defect concentration($[O_o'']_c$) which is:

$$[O_i'']_c=\frac{[O_i'']}{f} \quad (13)$$

where f is the site reduction factor, defined as the ratio of the number of available oxygen interstitial sites in doped urania to that in pure urania.

Since one Willis defect is created by introducing two oxygen interstitials, the chemical concentration of this defect is related to its absolute concentration by:

$$[(2:2:2)']_c=\frac{[(2:2:2)']}{f^2} \quad (14)$$

The site reduction factor, f in $Gd_zU_{1-z}O_{2\pm x}$ is defined as the following;

$$f=\exp(-\alpha z) \quad (15)$$

where α is the number of anion interstitial sites eliminated by introduction of one dopant ion. This is a general form which reduces to $f=1-\alpha z$ for small z values. Since one cation faces six nearby oxygen interstitial sites in the fluorite structure, α

should be about 6.

Substituting eq.(13) and eq.(14) into eqns.(7) and (12) in Table 1 yields:

$$\frac{[O_i''][U^{\cdot}]^2}{[U^x]P_o^{1/2}}=f\,K_{OX} \quad (16)$$

$$\frac{[O_i''][V_o^{\cdot\cdot}]}{[O_o^x]}=f\,K_F \quad (17)$$

Equations (8), (9), (10) and (11) do not change.

Since they are negatively charged, the Gd dopants(Gd_U') seem to attract anion vacancies and form dopant–vacancy clusters. Out of many possible clusters, the following reaction gives the best result:

$$V_o^{\cdot\cdot}+U_U^X+2Gd_U'+U^{\cdot}=(2U:V:2Gd)^{\cdot} \quad (18)$$

where $(2U:V:2Gd)^{\cdot}$ is the dopant–vacancy cluster.

Applying the mass action law to eq.(18) gives:

$$\frac{[(2U:V:2Gd)^{\cdot}]}{[V_o^{\cdot\cdot}][U_u^X][Gd_u']^2[U^{\cdot}]}=K_I \quad (19)$$

The site-filling conditions in the fluorite structure give:

$$[U_U^X]+[U^{\cdot}]+[U']+2[(2U:V:2Gd)^{\cdot}]=1 \quad (20)$$

$$[O_o^X]+[V_o^{\cdot\cdot}]+2[(V:U:V)^{\cdot\cdot}]+[(2U:V:2Gd)^{\cdot}]=2 \quad (21)$$

Specification of the parameter x characterizing the deviation from exact stoichiometry produces the equation:

$$[O_i'']+2[(2:2:2)']-[V_o^{\cdot\cdot}]$$
$$-2[(V:U:V)^{\cdot\cdot}]-[(2U:V:2Gd)^{\cdot}]=x \quad (22)$$

where x is in $Gd_zU_{1-z}O_{2+x}$. Finally, the charge neutrality gives:

$$[(2:2:2)']+2[O_i'']+[U']+z=2[(V:U:V)^{\cdot\cdot}]$$
$$+3[V_o^{\cdot\cdot}]+[U^{\cdot}]+3[(2U:V:2Gd)^{\cdot}] \quad (23)$$

Ⅳ. Calculation and Results

The model was fitted to the oxygen potential data for $(U,Gd)O_{2\pm x}$ from the works of Une and Oguma[10,12], and Lindemer and Sutton[11]. The nine equations– eqs.(9), (10), (11), (17), (19), (20), (21), (22), and (23)–were solved numerically to get the concentration of each defect. From eq.(8) or eq.(16), the equilibrium oxygen partial pressure was obtained from the calculated defect concentrations. The equilibrium constants except K_I found in pure urania (Table 4) were used in the calculation; however, achievement of satisfactory agreement between the data and the model required that α of eq.(15) and the equilibrium constant K_I in eq.(19) be adjusted at each temperature. The dopant cation fractions used in the analysis varied from z=0.1 to z=0.4.

Figures 1–3 show the best fits of the model to the data for three temperatures and several dopant concentrations. The curves representing the model are seen to agree quite well with the data over large ranges of x and z. The oxygen partial pressure increases with z. Of particular significance is the ability of the model to produce the sharp change in the oxygen potential at O/M=2. In the mixed-oxide model of Une and Oguma [10], the abrupt change in oxygen potential occurs when the average uranium valence is 4, not when O/M=2. These two conditions are identical in pure urania, but are different in the trivalent-doped urania.

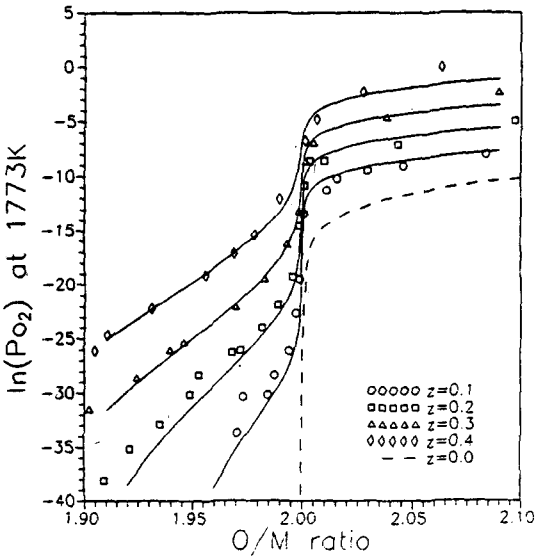

Fig. 1 Model Calculations (Curves) and Experimental Data (Points) [11] at 1773K.

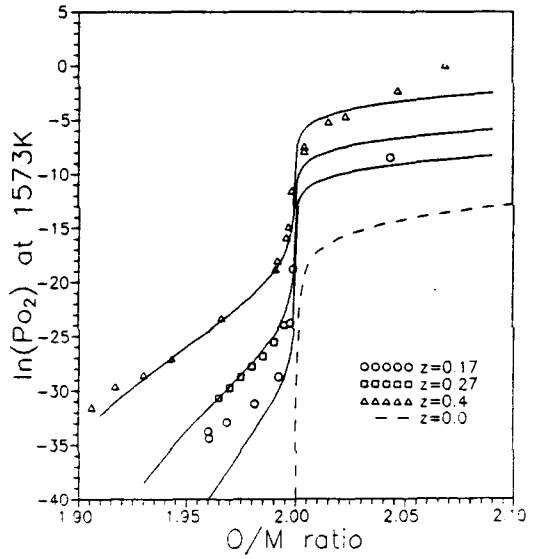

Fig. 2 Model Calculations (Curves) and Experimental Data (Points) [10] at 1573K.

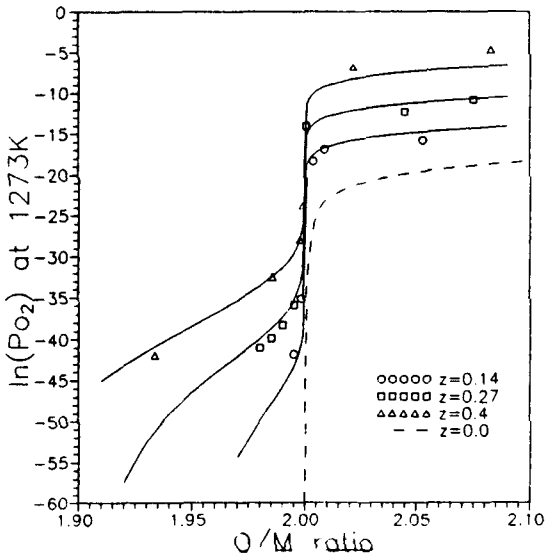

Fig. 3 Model Calculations (Curves) and Experimental Data (Points) [10, 12] at 1273K.

curves in Figs.1–3 are shown in Table 4. The values of K_F (S_F^O=5J/mol-K, H_F^O=355kJ/mol) which are lose to those determined by Kim and Olander[13] were used for the calculation purposes.

Table. 5 The Values of α and $\ln K_I$ Used in the Present Study.

T(K)	α	ln K_I
1273	10.0	13
1573	8.1	9
1773	6.5	7

Figs. 4 and 5 whow the model predictions of the concentrations of the various defects. Based on each defect behavior with the stoichiometry, we can examine simplified forms of the full set of equations. In the hyperstoichiometric region, Willis defects and holes are the major ones, while negative polarons, vacancies and vacancy dimers are negligible. In this case, $[(2:2:2:Y] \sim x/2$ and the full set of equations can be reduced to:

$$\ln P_{o2} \sim \ln x + \ln \frac{z}{4} + z\alpha - 2 \ln K_{OX} - \ln K_C \quad (24)$$

The comparable approximation to the oxygen pressure in the hypostoichiometric oxide can be shown to be:

$$\ln P_{o2} \sim 2\,|\ln (2z^3) - \ln x + \ln K_I + \ln K_F - \ln K_{OX}| \quad (25)$$

The significance of the approximations given by eqs.(24) and (25) is not in their accuracy in representing the data but in the parameters they contain. They show that the parameter α is determined primarily by the behavior of the oxygen potential in the hyperstoichiometric oxide, while K_I is important chiefly in fitting the oxygen potential data for the hypostoichiometric oxide.

Table 5 shows that the parameter α exhibits the expected value(about 6) at high temperature, but becomes larger as the temperature decreases. This may be due to thermal contraction of the lattice as the temperature decreases, which reduces the distance between the dopant ion and nearby oxygen interstitial sites. Since the Coulomb force responsible for the blocking action of Gd

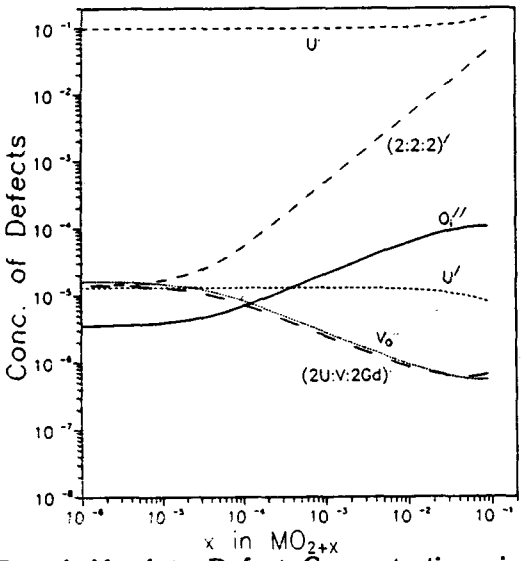

Fig. 4 Absolute Defect Concentrations in $Gd_{0.1}U_{0.9}O_{2-x}$ at 1773K.

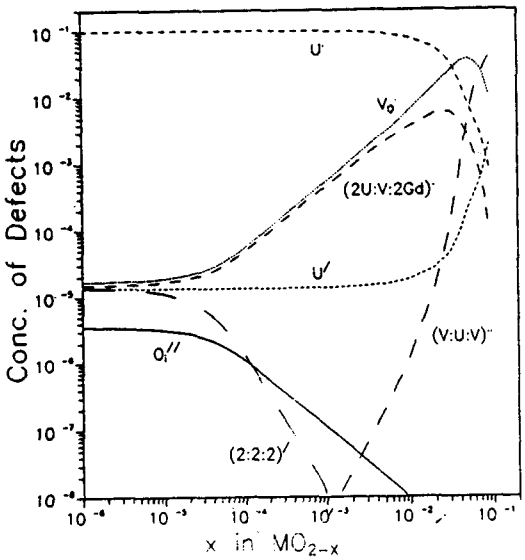

Fig. 5 Absolute defect concentrations in $Gd_{0.1}U_{0.9}O_{2-x}$ at 1773K.

dopants and oxygen interstitials are unaffected by temperature, the net result would be to bring more sites into the range of the repulsive interaction as the temperature decreases.

Based on the equilibrium consants in Table 5, the entropy and enthalpy change for the formation of the dopant–vacancy cluster are obtained as –68.3J/mol–K and –224.7kJ/mol, respectively. One of important characteristics of Gd–dopants is that they do not make extrinsic anion vacancies to meet the charge neutrality. The neutrality condition in this case is mainly met by the increased hole concentration. Gd–dopants do make dopant–vacancy clusters as the intrinsically–generated anion vacancy concentration increases with the non–stoichiometry of the oxide. However, the portion of the dopants contained in this cluster is very small, and most Gd–dopants exist as isolated defects. This kind of isolated defects is not rare. Tsuji et al., suggested a defect model where Ti exists as an isolated defect until the oxygen interstitial concentration becomes high enough to form a complex dopant cluster to explain the decrease of the oxygen potential when Ti is added to Urania[14]

This defect model seems sound and reasonable, based on the fact that this model agrees quite well with the ensemble of the experimental data, and that the site blocking parameter(α) is very close to that expected on geometrical grounds.

Figure 6 shows the expected oxygen–partial–pressure of urania containing 8 a/o gadolinia

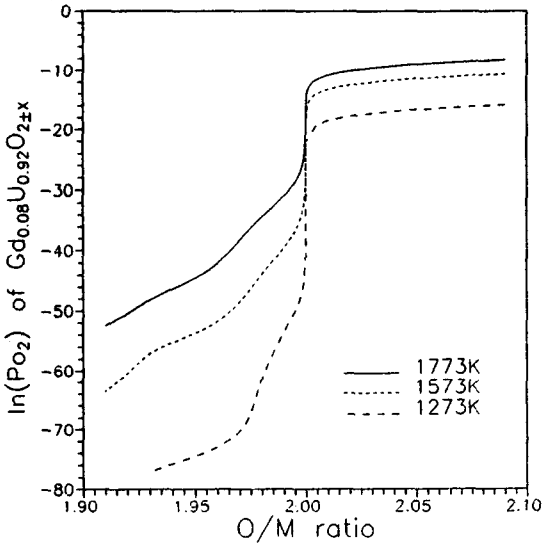

Fig. 6 Expected Oxygen Partial Pressures of $Gd_{0.08}1U_{0.92}O_{2\pm x}$ at 1773K, 1753K and 1273K.

which is used as the burnable poison in the nuclear reactor. Due to its ability to give the exact value of the oxygen potential at any given stoichiometry, this model can be very useful for the stoichiometry control of gadolinia doped urania during the sintering process.

V. Conclusions

A defect model of gadolinia doped urania has been developed on the foundation of the defect chemistry of pure urania. Using the available data, site reduction factors and the equilibrium constants for dopant–vacancy cluster formation were evaluated. This model quite well explains the behavior of the measured oxygen potential. Based on these facts, the following conclusions are obtained.

1. Gadolinium dopants in GDU exist mainly as isolate defects.
2. Gd dopants push away nearby oxygen interstitials. The number of eliminated oxygen interstitial sites per one dopant is about 6 which is close to that obtained from the geometrical ground. α becomes larger due to thermal contraction with decreasing temperature.
3. With increasing oxygen vacancies, Gd dopants form clusters where the number–ratio of the dopant and the vacancy is about 2. The entropy and enthalpy of the vacancy–dopant cluster formation are –16.4cal/mol–K and –53.9kcal/mol, respectively.

Acknowledgments

This work was supported by non–directional research fund by Korean Research Foundation.

References

1. Changhyo Kim et al., KAERI/NSC–387/89 (1989)
2. R. Manzel and W.O. Doerr, Amer. Ceram. Soc. Bull. 59(1980) 601
3. R. Eberle, H. Gross and W. Doerr, "Gadolinia Fuel Rods: Material Properties and Thermal Analysis", Enlarged Halden Program Group Meeting, Sonderstolen (1985)
4. O.T. Sorensen, "Nonstoichiometric Oxides", Academic Press (1981)
5. F.Schmittz, J. Nucl. Mater., 58 (1975) 357
6. C.R.A. Cattlow, J. Nucl. Mater., 67 (1977) 236
7. C.R.A. Cattlow and P.W. Tasker, Phil. Mag., 48 (1983) 649
8. J.H. Harding and R. Pandey, J. Nucl. Mater., 125 (1984) 125
9. K.Park and D.R. Olander, High Temp. Sci. 29 (1990) 203
10. K.Une and M.Oguma, J. Nucl. Mater., 110 (1982) 215
11. T.B. Lindemer and A.L. Sutton, J. Amer. Cer. Soc. 71 (1988) 553
12. K.Une and M.Oguma, J. Nucl. Mater., 118 (1983) 189
13. K.Kim and D.R.Olander, J.Nucl. Mater., 102 (1981) 192
14. T.Tsuji, T.Matsui, M.Abe and K.Naito, J. Nucl. Mater., 168 (1989) 151